

Effect of iso- and heterovalent cation substitutions on the superionic Faraday transition in fluorite-type modification β -PbF₂

© N.I. Sorokin

Shubnikov Institute of Crystallography „Crystallography and Photonics“, Russian Academy of Sciences, Moscow, Russia

E-mail: nsorokin1@yandex.ru

Received August 21, 2021

Revised August 21, 2021

Accepted April 4, 2022

The influence of isovalent substitutions of $\text{Pb}^{2+} \rightarrow \text{Cd}^{2+}$ and heterovalent substitutions of $\text{Pb}^{2+} \rightarrow \text{Sc}^{3+}$ on a superionic Faraday transition in $\text{Pb}_{1-x}\text{Cd}_x\text{F}_2$ ($x = 0.33$) and $\text{Pb}_{1-x}\text{Sc}_x\text{F}_{2+x}$ ($x = 0.1$) solid solutions based on the fluorite-type modification β -PbF₂ with sp. gr. $Fm\bar{3}m$ has been studied. The Faraday phase transition can be characterized by the temperature T_{tr}^λ corresponding to maximum on the heat capacity curve and temperature T_{tr}^α corresponding to the beginning of the structural disorder anion sublattice. Both of these temperatures are found on the temperature conductivity dependence $\sigma_{dc}(T)$ of β -PbF₂, $\text{Pb}_{0.67}\text{Cd}_{0.33}\text{F}_2$ and $\text{Pb}_{0.9}\text{Sc}_{0.1}\text{F}_{2.1}$ crystals. The values of T_{tr}^λ and T_{tr}^α in solid solutions compared with β -PbF₂ ($T_{tr}^\lambda = 715 \pm 10$ K, $T_{tr}^\alpha = 597 \pm 12$ K) decrease by 100–110 and 30–45 K for $\text{Pb}_{0.67}\text{Cd}_{0.33}\text{F}_2$ and $\text{Pb}_{0.9}\text{Sc}_{0.1}\text{F}_{2.1}$, respectively. Decreasing of temperature T_{tr}^λ leads to an increase in temperature interval of existence of the superionic state. For $T > T_{tr}^\lambda$ the anionic conductivity of fluorite-type $\text{Pb}_{0.67}\text{Cd}_{0.33}\text{F}_2$, $\text{Pb}_{0.9}\text{Sc}_{0.1}\text{F}_{2.1}$, and β -PbF₂ crystals reaches anomalously high values of $\sigma_{dc} = 1\text{--}2$ S/cm (873 K) at an ion transfer activation enthalpy equals to $H_\sigma \approx 0.3$ eV.

Keywords: phase transitions, fluorides, fluorite structure, ionic conductivity, solid solutions.

DOI: 10.21883/PSS.2022.07.54591.328

1. Introduction

A common feature of MF_2 ($M = \text{Ca}, \text{Sr}, \text{Ba}, \text{Cd}, \text{Pb}$) difluorides with a fluorite structure (structural type CaF_2), as well as crystals isostructural to them of other chemical classes (SrCl_2 , K_2S , Li_2O), is the existence of the Faraday [1,2] (first discovered by M. Faraday in PbF_2 in 1834 [3]) or in the terminology [4] diffuse phase transition shortly before the melting. Such a transition occurs without a change in symmetry (crystallographic group $Fm\bar{3}m$ of fluorite is retained), is initiated by the Coulomb interaction of charged defects, has a λ -like form of the temperature dependence of the heat capacity (on this basis, it is attributed to phase transitions of the II-th kind [5,6]).

The Faraday transition in MF_2 crystals is associated with a thermally activated process of structural disordering of the anionic sublattice. As a result of this transition, some of the F^- ions move from the main positions (tetrahedral in cations) to interstices (octahedral in cations and cubic in fluorine) and fluorine vacancies appear in the main anionic positions. Formation of anti-Frenkel pair defects in fluorite fluorides, consisting of an interstitial ion F_i' and a $\text{V}_\text{F}^\bullet$ vacancy (defects are denoted in Kroeger–Wink symbols [7]) is proved by various methods [8]. Due to the Faraday phase transition associated with the structural disorder of the anionic sublattice, MF_2 fluorite crystals have anomalously low melting heats and entropies [9,10].

The gradual disordering of the anionic sublattice is accompanied by the appearance of anionic conductivity in σ_{dc} in MF_2 crystals. The cation sublattice remains

ordered and does not participate in ion transport. During the Faraday transition, the degree of disordering of the anion sublattice is quite low (1–5% [9–13]), so the hopping model of charge carrier motion can be used to describe ion transport.

In the region of the Faraday transition on the Arrhenius plot $\lg \sigma_{dc} T - 1/T$ for fluorite crystals there is a bend towards a decrease in the enthalpy of activation of electrical conductivity H_σ . A jump in conductivity σ_{dc} during the transition was not detected. The Faraday transition temperature T_{tr} is usually determined based on the maximum on the temperature dependence of the heat capacity T_{tr}^λ [4], as well as based on the inflection point on the temperature dependence of the electrical conductivity [9,12], elastic constants [11] and other properties. Since the Faraday transition actually corresponds to a certain temperature range, the values T_{tr} found by various methods may differ from each other.

The Faraday diffuse transition refers to structural phase transitions of „order-disorder“ type, to which the thermally activated model of two-level systems is applicable [14,15]. When considering diffuse transitions in crystals, it is necessary to take into account the kinetics of the phase transformation. In the article [16] it is proposed to characterize the diffuse phase transition by two parameters: the temperature T_{tr}^λ corresponding to the maximum on the heat capacity curve and the temperature T_{tr}^α corresponding to the beginning of the structural disorder of the anionic sublattice. In this article, it is shown that both of these characteristic temperatures are found in the temperature

dependence of the ionic conductivity of MF_2 fluorite crystals. The difference $\Delta T_{tr} = T_{tr}^\lambda - T_{tr}^\alpha$ corresponds to the extension region of the Faraday transition and characterizes the phase transition kinetics.

Fluorite crystals MF_2 are characterized by two structural forms within one crystallographic group $Fm\bar{3}m$. At $T < T_{tr}^\alpha$, the ordered structural forms ht - MF_2 have an insignificant intrinsic ionic conductivity and are typical dielectrics. As temperature increases, the anti-Frenkel disordering of the anionic sublattice is accompanied by an increase in the ionic conductivity of MF_2 crystals. At $T > T_{tr}^\lambda$, the conductivity of the structurally-disordered forms of ht - MF_2 reaches $\sigma_{dc} \sim 1$ S/cm [17] values that are practically the same as in the molten state [18].

In the article [19] it was suggested that the structure of anionic sublattices of heterovalent solid solutions $M_{1-x}R_xF_{2+x}$ (R — rare-earth elements, room temperature) and structural modifications of ht - MF_2 crystals (high temperatures) are close. Studies of the defect structure of $M_{1-x}R_xF_{2+x}$ crystals are being actively conducted (references in reviews [20,21]). There are few high-temperature studies of the structural forms of ht - MF_2 crystals, and they have been carried out only for the fluorite modification β - PbF_2 [22,23]. Attempts to preserve the high-temperature disordered state ht - MF_2 to room temperature by heat treatment (quenching) method were unsuccessful. This makes it difficult to compare the defectiveness of anionic motifs of ht - MF_2 and $M_{1-x}R_xF_{2+x}$ crystals based on structural data.

In the context of what has been said, it is of interest to study Faraday phase transitions by the electrophysical method, since the electrical conductivity is directly related to the defectiveness of the anionic motif of fluorite crystals. For CaF_2 , SrF_2 , and BaF_2 crystals, such studies are hindered by high phase transition temperatures. In comparison with them, the fluorite modification β - PbF_2 is the most low-melting (melting point $T_{fus} = 1098 \pm 5$ K). For it, the maximum heat capacity temperatures according to different authors are 705 [24], 710 [25], 715 [26], 718 [27] and 721 K [28] (mean $T_{tr}^\lambda = 715 \pm 10$ K). The temperature T_{tr}^α corresponding to the beginning of the structural disorder of the anionic sublattice is 597 ± 12 K [16]. The temperature range of the Faraday transition is $\Delta T_{tr} = T_{tr}^\lambda - T_{tr}^\alpha \approx 120$ K. In case of the β - PbF_2 crystal, the temperature region of the phase transition is accessible to our experiment.

The issue of the effect of crystal doping on the Faraday transition was considered on the basis of an analysis of data obtained by thermal analysis and light scattering for $Ca_{1-x}Y_xF_{2+x}$ [29], $Ba_{1-x}La_xF_{2+x}$ [6,30], $Pb_{1-x}R_xF_{2+x}$ ($R = La, Yb$) [31] and $M_{1-x}U_xF_{2+2x}$ ($M = Ba, Pb$) [32] solid solutions. In these articles, it was found that, as a rule, an increase in the concentration of the impurity component leads to an expansion of the temperature interval for the existence of the superionic state of fluorite crystals.

The aim of this article was to analyze high-temperature data on the ionic conductivity of $Pb_{0.67}Cd_{0.33}F_2$ and $Pb_{0.9}Sc_{0.1}F_{2.1}$ solid solutions and to study the influence of isovalent (Pb^{2+} on Cd^{2+}) and heterovalent (Pb^{2+} on

Sc^{3+}) isomorphic substitutions for the superionic Faraday transition in the fluorite modification β - PbF_2 .

2. Growing single crystals and measuring the ionic conductivity of $Pb_{1-x}Cd_xF_2$ and $Pb_{1-x}Sc_xF_{2+x}$ solid solutions

In quasi-binary systems PbF_2 – CdF_2 and PbF_2 – ScF_3 [33] isovalent $Pb_{1-x}Cd_xF_2$ and heterovalent $Pb_{1-x}Sc_xF_{2+x}$ solid solutions with fluorite structure are formed. In the system PbF_2 – CdF_2 , a complete isomorphism of components ($0 \leq x \leq 1$) is implemented, while in the system PbF_2 – ScF_3 there is a partial isomorphism of components ($0 \leq x \leq 0.15$). Choice of compositions of the studied crystals $Pb_{0.67}Cd_{0.33}F_2$ (composition corresponds to the minimum on the melting curve) and $Pb_{0.9}Sc_{0.1}F_{2.1}$ is due to the fact that they have the maximum values σ_{dc} among $Pb_{1-x}Cd_xF_2$ and $Pb_{1-x}Sc_xF_{2+x}$ [34,35] solid solutions. For comparative analysis, we measured the electrical conductivity of a β - PbF_2 single crystal doped with a small amount of scandium.

Single crystals $Pb_{1-x}Cd_xF_2$ ($x = 0.33$), $Pb_{1-x}Sc_xF_{2+x}$ ($x = 0.1$) and β - PbF_2 were obtained from the melt by the method of directional Bridgman crystallization in graphite crucibles in a fluorinating atmosphere of polytetrafluoroethylene pyrolysis products [35–37]. The rate of crucible lowering in the growth zone was 3.5 mm/h, the cooling rate of the crystals was 50–100 K/min. The crystals did not contain light-scattering inclusions of oxygen-containing phases. The content of oxygen impurity in them was less than 10^{-3} mass.% [35]. The belonging of the grown crystals to the fluorite structural type (crystallographic group $Fm\bar{3}m$, $Z = 4$) was confirmed by X-ray diffractometers (HZG-4 and Philips PW1710 diffractometers, $CuK\alpha$ radiation, internal standard Si). Lattice cell parameters for cubic crystals $Pb_{0.67}Cd_{0.33}F_2$, $Pb_{0.9}Sc_{0.1}F_{2.1}$ and β - PbF_2 , (± 0.005 Å) are $a = 5.7575$, 5.875 and 5.940 Å respectively. The chemical composition of the $Pb_{0.67}Cd_{0.33}F_2$ and $Pb_{0.9}Sc_{0.1}F_{2.1}$ solid solutions corresponded to the composition of the initial charging: the discrepancies in the concentrations of the components (PbF_2 , CdF_2 , ScF_3) did not exceed ± 1 mol.%.

Ionic static conductivity σ_{dc} of crystals was determined by impedance spectroscopy in the frequency range 1 – 10^7 Hz (Solartron 1260 and Tesla BM-507 impedance meters). Single-crystal samples were not oriented with respect to the crystallographic axes, since they have cubic symmetry and there is no electrical conductivity anisotropy in them. The $\sigma_{dc}(T)$ dependences were measured in the range from room temperature (293 K) to 873 K in a nitrogen atmosphere N_2 or vacuum (~ 1 Pa). A detailed description of the experimental setups and the results of conductometric studies of crystals are published in [34,36–39].

3. Faraday phase transition in an isovalent $\text{Pb}_{1-x}\text{Cd}_x\text{F}_2$ ($x = 0.33$) solid solution

The temperature dependence of the ionic conductivity $\sigma_{dc}(T)$ for the isovalent $\text{Pb}_{0.67}\text{Cd}_{0.33}\text{F}_2$ solid solution is shown in Fig. 1. High-temperature anomaly is observed in the dependence $\sigma_{dc}(T)$, which is associated with the manifestation of the Faraday phase transition. Analysis of the data shows that the characteristic transition temperatures are $T_{tr}^{\lambda} \approx 620$ K and $T_{tr}^{\alpha} \approx 510$ K, the length of the transition is $\Delta T_{tr} \approx 110$ K. For comparison, Figure 1 shows the dependence $\sigma_{dc}(T)$ for the fluorite modification $\beta\text{-PbF}_2$ containing a small amount of scandium. In case of a $\beta\text{-PbF}_2$ crystal, the temperatures and length of the transition are $T_{tr}^{\lambda} \approx 720$ K, $T_{tr}^{\alpha} \approx 620$ K and $\Delta T_{tr} \approx 100$ K respectively. The results obtained for the $\beta\text{-PbF}_2$ crystal are in good agreement with the literature data [16,24–28].

In the $\text{Pb}_{0.67}\text{Cd}_{0.33}\text{F}_2$ solid solution compared to the $\beta\text{-PbF}_2$ matrix the values T_{tr}^{λ} and T_{tr}^{α} decrease by 100–110 K, which leads to an increase in the interval of existence of the high-temperature ht -phase down in temperature. A decrease in T_{tr}^{λ} and T_{tr}^{α} values was also observed by thermal analysis for a solid solution of similar composition $\text{Pb}_{0.6}\text{Cd}_{0.4}\text{F}_2$ [26], for which the Faraday transition occurs in the temperature range 400–600 K.

In intervals $T < T_{tr}^{\alpha}$ and $T > T_{tr}^{\lambda}$ conductometric data for $\text{Pb}_{0.67}\text{Cd}_{0.33}\text{F}_2$ and $\beta\text{-PbF}_2$ satisfy the Arrhenius–Frenkel equation:

$$\sigma_{dc}T = \sigma_0 \exp(-H_{\sigma}/kT),$$

where σ_0 is the pre-exponential conductivity multiplier and H_{σ} is the activation enthalpy of ion transport. The parameters σ_0 and H_{σ} are provided in Table 1.

When comparing low-temperature forms $lt\text{-Pb}_{0.67}\text{Cd}_{0.33}\text{F}_2$ and $lt\text{-}\beta\text{-PbF}_2$ it can be seen that the conductivity of the solid solution is much higher than that of the matrix (Table 2). In high temperature forms $ht\text{-Pb}_{0.67}\text{Cd}_{0.33}\text{F}_2$ and $ht\text{-}\beta\text{-PbF}_2$, the $\sigma_{dc}(T)$ curve reaches the level of abnormally high ionic conductivity and the ion transport parameters are close: $\sigma_{dc} = 1\text{--}2$ S/cm (873 K) and $H_{\sigma} = 0.29 \pm 0.02$ eV. The obtained enthalpy H_{σ} for the $\beta\text{-PbF}_2$ crystal is confirmed by neutron diffraction methods (0.26 eV [13]), magnetic resonance on nuclei ^{19}F (0.2 eV [40]) and conductometry (0.25–0.3 eV [17]).

However, the reasons for the appearance of superionic conductivity comparable to σ_{dc} of their melts in high-temperature states of $ht\text{-Pb}_{0.67}\text{Cd}_{0.33}\text{F}_2$ and $ht\text{-}\beta\text{-PbF}_2$ crystals are different. In $\beta\text{-PbF}_2$ the temperature increase is accompanied by a rapid increase in the concentration of charge carriers — anti-Frenkel defects F_i' and V_F^{\bullet} . As the temperature lowers, thermally activated defects annihilate, and the crystal becomes an insulator.

In $\text{Pb}_{0.67}\text{Cd}_{0.33}\text{F}_2$, the main reason for the appearance of superionic conductivity is isovalent isomorphic substitutions of Pb^{2+} for Cd^{2+} . Isovalent isomorphism with the formation of solid solutions is one of the methods for controlling

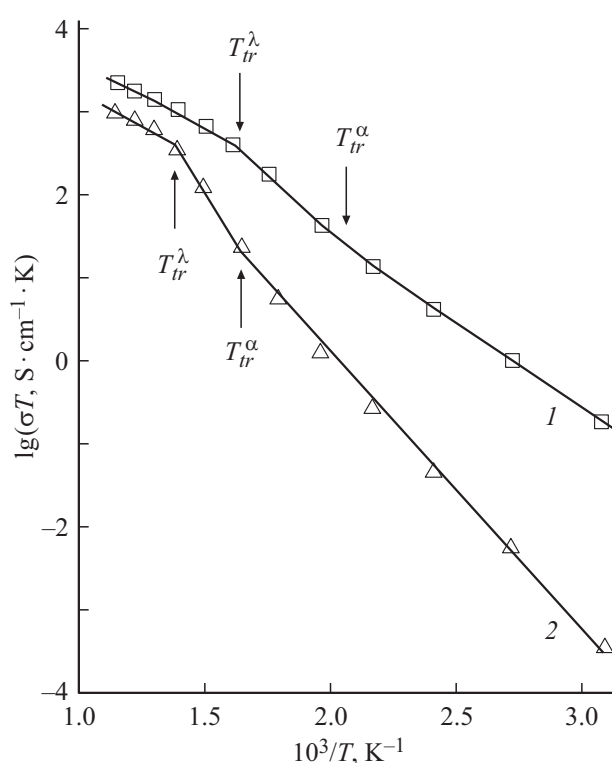


Figure 1. Temperature dependence of ionic conductivity for (1) isovalent solid solution $\text{Pb}_{0.67}\text{Cd}_{0.33}\text{F}_2$ ($T_{tr}^{alpha} \approx 510$ K and $T_{tr}^{\lambda} \approx 620$ K) and (2) fluorite matrix $\beta\text{-PbF}_2$ ($T_{tr}^{\alpha} \approx 620$ K and $T_{tr}^{\lambda} \approx 720$ K) in the Faraday region phase transition.

the electrophysical properties of fluoride materials. Due to the equality of the charges of the substituting cations, it does not lead to the formation of additional charged point defects and, as a rule, to strong changes in the crystal properties. Isovalent isomorphism of fluorite solid solutions in the $\text{PbF}_2\text{--CdF}_2$ system is an exception and differs greatly from the $\text{MF}_2\text{--}M'\text{F}_2$ systems formed by fluorides of alkaline earth elements ($M = \text{Ca, Sr and Ba}$). This is due to the difference in the band electronic structure of lead and cadmium difluorides from the fluorides of alkaline earth elements, as well as the large difference in the ionic radii of Pb^{2+} (1.43 Å) and Cd^{2+} (1.24 Å for coordination number 8 [41]).

X-ray diffraction analysis of $\text{Pb}_{0.67}\text{Cd}_{0.33}\text{F}_2$ [42] crystals revealed a high concentration of anion vacancies V_F^{\bullet} even at room temperature, which is $25 \pm 2\%$ in the main anionic positions, and the corresponding number of interstitial ions F_i' . „Crystallochemical“ anti-Frenkel defects ($F_i' + V_F^{\bullet}$) caused by Pb^{2+} substitutions for Cd^{2+} , are retained with decreasing temperature, in contrast to thermally stimulated anti-Frenkel defects [8] in the matrix $\beta\text{-PbF}_2$.

In the article [38] the concentration of charge carriers (interstitial F_i' ions) in $\text{Pb}_{0.67}\text{Cd}_{0.33}\text{F}_2$ crystals is determined which is equal to $5.1 \cdot 10^{21} \text{ cm}^{-3}$. Then the calculated mobility of charge carriers at 873 K is:

$$\mu_{Fi} = \sigma_{dc}/qn_{\text{mob}} = 3.1 \cdot 10^{-3} \text{ cm}^2/\text{Vs}.$$

Table 1. Characteristic temperatures T_{tr}^{α} and T_{tr}^{λ} , multiplier σ_0 and activation enthalpy of conductivity H_{σ} in low- (*lt*) and high-temperature (*ht*) forms of $\text{Pb}_{0.67}\text{Cd}_{0.33}\text{F}_2$, $\text{Pb}_{0.9}\text{Sc}_{0.1}\text{F}_{2.1}$ and $\beta\text{-PbF}_2$ crystals

Crystal	T_{tr}^{α} , K	T_{tr}^{λ} , K	Structural form	σ_0 , SK/cm	H_{σ} , eV
$\text{Pb}_{0.67}\text{Cd}_{0.33}\text{F}_2$	510	620	<i>lt</i>	$4.5 \cdot 10^5$	0.410(2)
			<i>ht</i>	$2.5 \cdot 10^5$ [38] $1.5 \cdot 10^5$	0.39 [38] 0.314(7)
$\text{Pb}_{0.9}\text{Sc}_{0.1}\text{F}_{2.1}$	570	670	<i>lt</i>	$4.4 \cdot 10^5$	0.423(2)
			<i>ht</i>	$2.5 \cdot 10^5$ [37] $5.1 \cdot 10^4$	0.39 [37] 0.290(4)
$\beta\text{-PbF}_2$	620 597 ± 12 [16]	720 715 ± 10 K [24–28]	<i>lt</i>	$3.7 \cdot 10^6$	0.642(5)
			<i>ht</i>	$3.5 \cdot 10^4$	0.267(5)

Table 2. Ionic conductivity, concentration and mobility of charge carriers in the $\beta\text{-PbF}_2$ fluorite matrix and solid solutions based on it at 323 K ($T < T_{tr}^{\alpha}$) and 873 K ($T > T_{tr}^{\alpha}$)

Properties	β -PbF ₂		Pb _{0.67} Cd _{0.33} F ₂		Pb _{0.9} Sc _{0.1} F _{2.1}	
	$T < T_{tr}^{\alpha}$	$T > T_{tr}^{\lambda}$	$T < T_{tr}^{\alpha}$	$T > T_{tr}^{\lambda}$	$T < T_{tr}^{\alpha}$	$T > T_{tr}^{\lambda}$
σ_{dc} , S/cm	$1.2 \cdot 10^{-6}$	1.2	$5.9 \cdot 10^{-4}$	2.5	$3.6 \cdot 10^{-4}$	1.2
n_{mob} , cm ⁻³	$2.2 \cdot 10^{16}$ *	$2 \cdot 10^{20}$ ***	$5.1 \cdot 10^{21}$ [37]		$2 \cdot 10^{21}$ [36]	
μ_{mob} , cm ² /Vs	$7.3 \cdot 10^{-8}$ (F' _i) *	$8.7 \cdot 10^{-3}$ (F' _i) ***	$7.2 \cdot 10^{-7}$	$3.1 \cdot 10^{-3}$	$1.1 \cdot 10^{-6}$	$3.7 \cdot 10^{-3}$
	$6.4 \cdot 10^{-8}$ (F' _i) **	$2.3 \cdot 10^{-3}$ (V [•] _F) ***				
	$4.3 \cdot 10^{-5}$ (V [•] _F) *					
	$8.1 \cdot 10^{-6}$ (V [•] _F) **					

Note. * — data from [47] at 323 K, ** — data from [48] at 323 K and *** — data from [2] at 780 K.

The ionic conductivity of $\beta\text{-PbF}_2$ crystals depends on uncontrolled impurities and thermal history (different cooling modes) [43]. According to [2] at the Faraday transition (780 K, at the beginning of the negative deviation of the $\sigma_{dc}(T)$ curve from the Arrhenian behavior when cooling), the characteristics of charge carriers in a nominally pure crystal $\beta\text{-PbF}_2$ are: the concentration of anti-Frenkel pairs $n_{\text{AF}} = 2.0 \cdot 10^{20} \text{ cm}^{-3}$, mobility of defects $\mu_{VF} = 2.3 \cdot 10^{-3}$ and $\mu_{Fi} = 8.7 \cdot 10^{-3} \text{ cm}^2/\text{Vs}$. It can be seen that at $T > T_{tr}^{\lambda}$ the mobility of defects in the solid solution is of the same order as the mobility of anti-Frenkel defects in the matrix.

4. Faraday phase transition in a heterovalent solid solution $\text{Pb}_{1-x}\text{Sc}_x\text{F}_{2+x}$ ($x = 0.1$)

The temperature dependence of conductivity $\sigma_{dc}(T)$ for the heterovalent solid solution $\text{Pb}_{0.9}\text{Sc}_{0.1}\text{F}_{2.1}$ is shown in Fig. 2. The deviation of the $\sigma_{dc}(T)$ dependence from the Arrhenian behavior is observed in the temperature range 570–670 K ($T_{tr}^{\lambda} \approx 670$ K and $T_{tr}^{\alpha} \approx 570$ K). The length of the phase transition is $\Delta T_{tr} \approx 100$ K. Decrease in T_{tr}^{λ} and T_{tr}^{α} values in $\text{Pb}_{0.9}\text{Sc}_{0.1}\text{F}_{2.1}$ solid solution compared to the

$\beta\text{-PbF}_2$ matrix is 30–45 K. In the temperature intervals $T < T_{tr}^{\alpha}$ and $T > T_{tr}^{\lambda}$, the conductometric data satisfy the Arrhenius–Frenkel equation, the parameters σ_0 and H_{σ} are provided in Table 1.

It can be seen that in the low-temperature form of the *lt*- $\text{Pb}_{0.9}\text{Sc}_{0.1}\text{F}_{2.1}$ solid solution, the values of $\sigma_{dc}(T)$ are also significantly higher than in *lt*- $\beta\text{-PbF}_2$ (Table 2). At $T > T_{tr}^{\lambda}$, the $\sigma_{dc}(T)$ curve reaches the level of superionic conductivity 0.1–2 S/cm. In high-temperature *ht*-forms, superionic transport parameters coincide in $\text{Pb}_{0.9}\text{Sc}_{0.1}\text{F}_{2.1}$ and $\beta\text{-PbF}_2$ crystals (crystals were grown under identical conditions in the same growth experiment).

The reason for the appearance of high superionic conductivity in the high-temperature *ht*- $\text{Pb}_{1-x}\text{Sc}_x\text{F}_{2+x}$ state differs from the situation in the *ht*- $\beta\text{-PbF}_2$ and *ht*- $\text{Pb}_{0.67}\text{Cd}_{0.33}\text{F}_2$ crystals. In $\text{Pb}_{1-x}\text{Sc}_x\text{F}_{2+x}$ crystals, the factor of temperature increase is superimposed by an additional factor of change in the chemical composition caused by heterovalent substitutions of Pb^{2+} on Sc^{3+} . When Pb^{2+} is substituted for Sc^{3+} , interstitial ions F_i' appear, disturbing the stoichiometry of the $\beta\text{-PbF}_2$ matrix. Crystal chemical anionic defects caused by a change in the composition of $\text{Pb}_{0.9}\text{Sc}_{0.1}\text{F}_{2.1}$ are retained when the temperature is lowered to room temperature. Unfortunately, the defect structure of the $\text{Pb}_{0.9}\text{Sc}_{0.1}\text{F}_{2.1}$

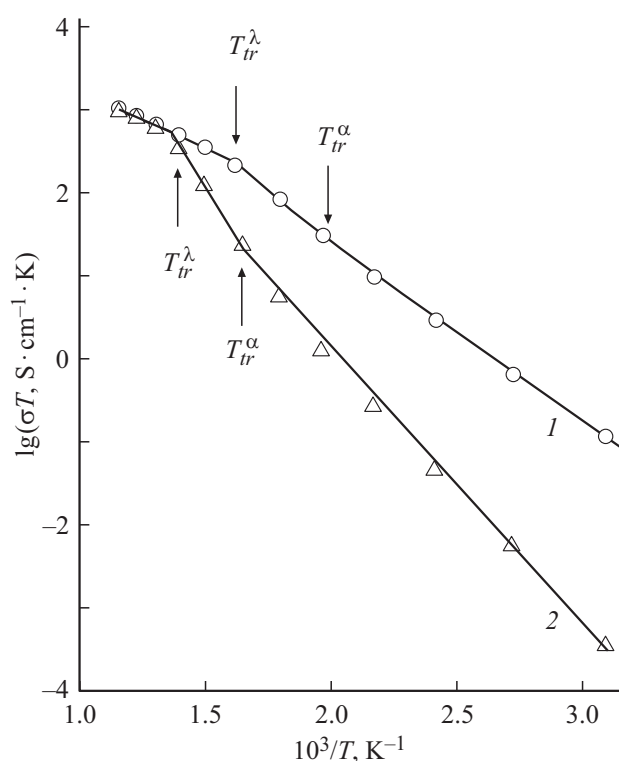


Figure 2. Temperature dependence of ionic conductivity for (1) heterovalent solid solution $\text{Pb}_{0.9}\text{Sc}_{0.1}\text{F}_{2.1}$ ($T_{tr}^{\alpha} \approx 570$ K and $T_{tr}^{\lambda} \approx 670$ K) and (2) fluorite matrix $\beta\text{-PbF}_2$ ($T_{tr}^{\alpha} \approx 620$ K and $T_{tr}^{\lambda} \approx 720$ K) in the Faraday region phase transition.

fluorite solid solution has not been studied. However, in structural studies of fluorite crystals $M_{1-x}R_x\text{F}_{2+x}$ ($M = \text{Ca}, \text{Sr}, \text{Ba}$; $R = \text{La-Lu}, \text{Y}$) (references in [20,44]), and high-pressure fluorite phase $\text{Pb}_{0.3}\text{La}_{0.7}\text{F}_{2.7}$ [45] interstitial ions F_i' were found.

Concentration and mobility of charge carriers (interstitial ions F_i') in $\text{Pb}_{0.9}\text{Sc}_{0.1}\text{F}_{2.1}$ crystals were estimated in [37] which are $n_{\text{mob}} = 2.0 \cdot 10^{21} \text{ cm}^{-3}$ and $\mu_{\text{Fi}} = 3.7 \cdot 10^{-3} \text{ cm}^2/\text{Vs}$ (at 873 K), respectively. The mobility of defects in the solid solution is of the same order as the mobility of anti-Frenkel defects in the $\beta\text{-PbF}_2$ matrix (Table 2).

The decrease in the Faraday transition temperature is confirmed by the experimental results of measurements of the elastic compliance coefficients of $\text{Ca}_{0.91}\text{Y}_{0.09}\text{F}_{2.09}$ [29] and $\text{Ba}_{0.607}\text{La}_{0.393}\text{F}_{2.393}$ [11] crystals, heat capacity measurements of $\text{Pb}_{1-x}\text{R}_x\text{F}_{2+2x}$ ($R = \text{La}, \text{Yb}$ crystals ($R = \text{La}, \text{Yb}$; $0 < x < 0.17$) [31] and $\text{M}_{1-x}\text{U}_x\text{F}_{2+2x}$ ($M = \text{Ba}, \text{Pb}$; $0 < x < 0.10$) [46], as well as theoretical calculations [15]. The Faraday transition occurs at substantially lower temperatures in solid solutions than in fluorite matrices.

Theoretical calculations [29] indicate a relationship between temperature T_{tr} and the critical concentration of mobile defects (associated with the presence of interstitial fluorine ions and rare-earth cations), while data on conductivity [9] — with critical mobility of defects. The accelerated

ionic motion model („enhanced ionic motion“ model) [30] provides a reasonable explanation of the impurity effect on T_{tr} in $\text{M}_{1-x}\text{R}_x\text{F}_{2+x}$ crystals.

5. Conclusion

It is shown that the temperatures of the Faraday phase transition T_{tr}^{λ} (corresponding to the maximum on the heat capacity curve) and T_{tr}^{α} (corresponding to the beginning of structural disordering of the anionic sublattice) are found on the temperature dependences of ionic conductivity $\sigma_{dc}(T)$ for $\text{Pb}_{0.67}\text{Cd}_{0.33}\text{F}_2$ and $\text{Pb}_{0.9}\text{Sc}_{0.1}\text{F}_{2.1}$ fluorite solid solutions.

The effect of iso- and heterovalent isomorphism on the diffuse phase transition in MF_2 crystals with a fluorite structure is traced using $\beta\text{-PbF}_2$ as an example. The isomorphous introduction of isovalent (Cd^{2+}) and heterovalent (Sc^{3+}) cations lowers the temperatures T_{tr}^{λ} and T_{tr}^{α} in fluorite solid solutions compared to the one-component $\beta\text{-PbF}_2$ matrix by 30–45 and 100–110 K for $\text{Pb}_{0.9}\text{Sc}_{0.1}\text{F}_{2.1}$ and $\text{Pb}_{0.67}\text{Cd}_{0.33}\text{F}_2$ respectively. The introduction of additives (Cd^{2+} , Sc^{3+}) enables to expand downward the region of existence of the high-temperature superionic phase, for which abnormally high values of fluorine-ionic conductivity $\sigma_{dc} = 1\text{--}2 \text{ S/cm}$ (873 K) are achieved at the ion transport activation enthalpy $\Delta H_{\sigma} \approx 0.3 \text{ eV}$.

Comparison of charge carrier concentrations in $\text{Pb}_{0.67}\text{Cd}_{0.33}\text{F}_2$ and $\text{Pb}_{0.9}\text{Sc}_{0.1}\text{F}_{2.1}$ solid solutions with the concentration of thermally activated charge carriers in the high-temperature form $ht\text{-}\beta\text{-PbF}_2$ (at $T = T_{tr}^{\lambda}$) shows that they differ within an order. This indicates the structural disorder of the anionic sublattice in crystals $\text{Pb}_{0.67}\text{Cd}_{0.33}\text{F}_2$, $\text{Pb}_{0.9}\text{Sc}_{0.1}\text{F}_{2.1}$ (room temperature) and $ht\text{-}\beta\text{-PbF}_2$ (high temperatures). The obtained data on electrical conductivity confirm the assumption made in the article [19] that the anionic sublattice of $\text{Pb}_{1-x}\text{Cd}_x\text{F}_2$ and $\text{Pb}_{1-x}\text{Sc}_x\text{F}_{2+x}$ solid solutions can be represented as a high-temperature disordered (by anions) form $ht\text{-}\beta\text{-PbF}_2$ stabilized by isomorphous substitutions.

In high-temperature $ht\text{-}$ crystal forms $\beta\text{-PbF}_2$, $\text{Pb}_{0.67}\text{Cd}_{0.33}\text{F}_2$ and $\text{Pb}_{0.9}\text{Sc}_{0.1}\text{F}_{2.1}$, superion transport parameters are close. The result of isovalent ($\text{Pb}^{2+} \rightarrow \text{Cd}^{2+}$) and heterovalent ($\text{Pb}^{2+} \rightarrow \text{Sc}^{3+}$) substitutions is the preservation of the disordered defect state of the anion motif of solid solutions at room temperature. Structural disordering of the anionic sublattice determines the concentration contribution of n_{mob} to the conductivity σ_{dc} . Therefore, we can assume that „the ancestor“ of these solid solutions is the high-temperature form $ht\text{-}\beta\text{-PbF}_2$.

Significant concentrations of anionic defects in solid solutions appear even at room temperature. This leads to an increase in their cooperative interaction, to a strong anharmonicity of anion vibrations, to a mass displacement of anions from crystallographic positions, and to the possibility of the formation of structural clusters consisting of anionic and cationic defects. Heating is required to increase the mobility of anionic defects.

Isovalent ($\text{Pb}^{2+} \rightarrow \text{Cd}^{2+}$) and heterovalent ($\text{Pb}^{2+} \rightarrow \text{Sc}^{3+}$) substitutions in the fluorite modification $\beta\text{-PbF}_2$ lead to a decrease in the Faraday transition in temperature and to an extension of the temperature range for a state with abnormally high ionic conductivity $\sigma_{dc} > 0.1\text{--}2\text{ S/cm}$. High ionic conductivity is achieved by the combined action of two variables in the equation $\sigma_{dc} \sim n_{\text{mob}}\mu_{\text{mob}}$. Firstly, charge carriers appear due to structural disordering of the anionic sublattice due to isomorphic substitutions (concentration factor) and, secondly, high values of charge carrier mobility are achieved at lower temperatures due to the reduction of potential barriers to the migration of charge carriers (mobility factor).

During the Faraday phase transition, the conductivity σ_{dc} does not experience a jump, and the concentration and mobility of charge carriers change only slightly.

Funding

This work was supported by the Ministry of Science and Higher Education within the scope of the State Assignment of the Federal Scientific-Research Center „Crystallography and Photonics“ of the Russian Academy of Sciences.

Acknowledgments

The author is grateful to I.I. Buchinskaya for growing crystals and to B.P. Sobolev for discussing the article.

Conflict of interest

The author declares that he has no conflict of interest.

References

- [1] M. O’Keeffe. Superionic Conductors. / Eds G.D. Mahan et al. Plenum Press, N.Y. (1976) P. 101.
- [2] J. Schoonman. Fast ion transport in solids. / Eds P. Vashishta, J.N. Mundy, G.K. Shenoy. North-Holland, N.Y. (1979) P. 631.
- [3] M. Faraday. Experimental Researches in Electricity. Art. 1339. Taylor & Francis, London (1839).
- [4] A.S. Dworkin, M.A. Bredig. J. Phys. Chem. **72**, 1277 (1968).
- [5] V.R. Belosludov, R.I. Efremova, E.V. Matizen. FTT **16**, 1311 (1974) (in Russian).
- [6] V.N. Chebotin, V.I. Tsidilkovskii. Elektrokhimiya, **16**, 651 (1980) (in Russian).
- [7] F.A. Kroger. The chemistry of imperfect crystals. Amsterdam: North-Holland (1964). 1039 p.
- [8] A.B. Lidiard. Crystals with the Fluorite Structure / Ed. W. Hayes. Clarendon Press, Oxford. (1974). P. 101.
- [9] J. Schoonman. Solid State Ionics **1**, 121 (1980).
- [10] C.E. Derrington, A. Linder, M. O’Keeffe. J. Solid State Chem. **15**, 171 (1975).
- [11] P.E. Ngoepe, J.D. Comins. J. Phys. C **19**, L267 (1986).
- [12] A.V. Chadwick. Solid State Ionics **8**, 209 (1983).
- [13] R. Bachmann, H. Schulz. Solid State Ionics **9–10**, 521 (1983).
- [14] J. Oberschmidt. Phys. Rev. B **23**, 5038 (1981).
- [15] J.E. Vlieg, H.W. den Hartog, M. Winnick. J. Phys. Chem. Solids **47**, 521 (1986).
- [16] J. Eapen, A. Annamareddy. Ionics **23**, 1043 (2017).
- [17] A. Azimi, V.M. Carr, A.V. Chadwick, F.G. Kirkwood, R. Saghafian. J. Phys. Chem. Solids **45**, 23 (1984).
- [18] B.M. Voronin, S.V. Volkov. J. Phys. Chem. Solids **62**, 1349 (2001).
- [19] P.P. Fedorov, B.P. Sobolev. J. Less-Common Met. **63**, 31 (1979).
- [20] B.P. Sobolev. The rare earth trifluorides. Pt II. Introduction to materials science of multicomponent metal fluoride crystals. / Institute of Crystallography, Barcelona (2001). 460 p.
- [21] N.I. Sorokin, A.M. Golubev, B.P. Sobolev. Kristallografiya **59**, 275 (2014) (in Russian).
- [22] S.M. Shapiro, F. Reidinger. Physics of Superionic Conductors. / Ed. M.B. Salamon. Springer, Berlin (1979). P. 45.
- [23] K. Koto, H. Schulz, R.A. Huggins. Solid State Ionics **3–4**, 381 (1981).
- [24] C.E. Derrington, A. Navrotsky, M. O’Keeffe. Solid State Commun. **18**, 47 (1976).
- [25] J.P. Goff, W. Hayes, S. Hull, M.T. Hutching. J. Phys.: Condens. Matter. **3**, 3677 (1991).
- [26] I. Kosacki, A.P. Litvinchuk, J.J. Tarasov, M.Ya. Valakh. J. Phys.: Condens. Matter. **1**, 929 (1989).
- [27] L.M. Volodkovich, G.S. Petrov, R.A. Vechev, A.A. Vechev. Termochim. Acta **88**, 497 (1985).
- [28] M. Ouwerkerk. Mater. Res. Bull. **20**, 501 (1985).
- [29] C.R.A. Catlow, J.D. Comins, F.A. Germano, R.T. Harley, W. Hayes, I.B. Owen. J. Phys. C: Solid State Phys. **14**, 329 (1981).
- [30] J. Schoonman. Solid State Ionics **5**, 71 (1981).
- [31] H.W. den Hartog, J. van der Veen. Phys. Rev. B **37**, 1807 (1988).
- [32] M. Ouwerkerk, J. Schoonman. Solid State Ionics **12**, 479 (1984).
- [33] I.I. Buchinskaya, P.P. Fedorov. Uspekhi khimii **73**, 404 (2004) (in Russian).
- [34] N.I. Sorokin, I.I. Buchinskaya, B.P. Sobolev. ZhNKh **37**, 2653 (1992) (in Russian).
- [35] V. Trnovcova, P.P. Fedorov, I.I. Buchinskaya, V. Smatko, F. Hanic. Solid State Ionics **119**, 181 (1989).
- [36] N.I. Sorokin, P.P. Fedorov, B.P. Sobolev. Neorgan. materialy **33**, 5 (1997) (in Russian).
- [37] N.I. Sorokin. FTT **60**, 710 (2018) (in Russian).
- [38] N.I. Sorokin. FTT **57**, 1325 (2015) (in Russian).
- [39] N.I. Sorokin, B.P. Sobolev, M. Breiter. FTT **44**, 1506 (2002) (in Russian).
- [40] R.E. Gordon, J.H. Strange. J. Phys. C **11**, 3213 (1978).
- [41] R.D. Shannon. Acta Crystallogr. A **32**, 751 (1976).
- [42] V. Trnovcova, P.P. Fedorov, M. Ozvoldova, I.I. Buchinskaya, E.A. Zhurova. J. Optoelectron. Adv. Mater. **5**, 627 (2003).
- [43] Y. Ito, K. Koto, S. Yoshikado, T. Ohachi. Solid State Ionics **15**, 253 (1985).
- [44] S. Hull. Rep. Prog. Phys. **67**, 1233 (2004).
- [45] L.P. Otroschenko, V.B. Aleksandrov, N.A. Bendeleani, I.A. Verin, B.P. Sobolev. Kristallografiya **37**, 405 (1992) (in Russian).
- [46] M. Ouwerkerk, E.M. Kelder, J. Schoonman, J.C. van Miltenburg. Solid State Ionics **9–10**, 531 (1983).
- [47] R.W. Bonne, J. Schoonman. J. Electrochem. Soc.: Electrochem. Sci. Techn. **124**, 28 (1977).
- [48] I.V. Murin, A.V. Glumov, O.V. Glumov. Elektrokhimiya, **15** (1119), 1979 (in Russian).